PROCEEDINGS OF ECOS 2023 - THE 36TH INTERNATIONAL CONFERENCE ON
EFFICIENCY, COST, OPTIMIZATION, SIMULATION AND ENVIRONMENTAL IMPACT OF ENERGY SYSTEMS
25-30 JUNE 2023, LAS PALMAS DE GRAN CANARIA, SPAIN

A fast heuristic algorithm for multi-energy system design

Antoine Mallégol[a], Arwa Khannoussi[b], Mehrdad Mohammadi[c], Bruno Lacarrière[d], Patrick Meyer[c]

[a] *IMT Atlantique, Lab-STICC, UMR CNRS 6285, F-29238 Brest, France, antoine.mallegol@imt-atlantique.fr, CA*
[b] *IMT Atlantique, LS2N, UMR CNRS 6004, F-44307 Nantes, France,*
[c] *IMT Atlantique, Lab-STICC, UMR CNRS 6285, F-29238 Brest, France,*
[d] *IMT Atlantique, GEPEA, UMR CNRS 6144, F-44307 Nantes, France*

Abstract:

The optimization of multi-energy systems (MESs) in which multiple energy carriers interact with each other is a complex problem. Their optimal operation and design can be determined through mathematical programming. A classical technology used in MESs is the combined heat and power units (CHP) whose efficiency is modeled through non-linear equations. These non-linear functions are approximated through piecewise linear ones by introducing binary decision variables, which generates a mixed-integer linear program (MILP). Consequently, optimizing such systems over a long time period with a high temporal resolution becomes infeasible in a reasonable amount of time. In this work, we propose a fast heuristic algorithm to optimize the design and operation of such an MES. Our case study is an MES at the scale of a district with five types of generation units, including a CHP, over a time period of one year with a temporal resolution of one hour. Comparison of the proposed heuristic and a state-of-the-art MILP solver over smaller time periods shows that the heuristic is up to 99.9 % faster, with a mean error of 2.3×10^{-4} % compared to the optimal solution. The heuristic can also solve the optimal design and operation problem over a year in about 10 minutes.

Keywords:

Combined Heat and Power, Part-Load Efficiency, Heuristic, Linearization, Multi-Objective Optimization.

1. Introduction

Energy systems may include several types of energy carriers, such as electricity or heat. However, these carriers are classically considered as separate systems. Combining them into a single multi-energy system (MES) can increase the energy efficiency of the system by taking advantage of the synergies and interactions between the energy carriers [1]. It helps to reduce costs or reduce environmental impact by integrating renewable energy sources (RES) more easily in the form of intermittent energy sources [2].

An MES can be optimized using techniques from Operational Research by modeling the system as a mathematical program. Optimization of an MES generally focuses on improving two main areas of the system: its *design*, and its *operation*. Optimizing the design aims to select which production technologies to use in the system, along with their installed capacity, configuration, etc. Optimizing the operation deals with planning the use of the technologies to meet the energy demands by choosing at each time step how much energy each technology produces [3].

Two important points to consider when optimizing an MES are the time horizon and the temporal resolution of the optimization problem [4]. A large time horizon is more accurate to optimize the design, but more complex to solve. Similarly, high temporal resolution impacts the accuracy, especially when intermittent RES are considered in the system [5].

Two main approaches are typically used to solve such optimization problems: *exact* or *approximate* methods. Exact methods (e.g., branch-and-bound) solve the problem to optimality; however, they are computationally expensive and may not be able to even solve medium and large instances of the problem due to the high complexity of MES models. [6] review different exact methods and their properties to solve an MES. On the other hand, approximate methods employ approximate algorithms (e.g., heuristics or metaheuristics) to solve the problem. As their name implies, the approximate algorithms do not guarantee optimality but are able to provide good solutions (i.e., close to optimal) in a reasonable computation time for complex MES models. As an example, [7] use Particle Swarm Optimization algorithm, as a metaheuristic algorithm, to minimize the cost of an MES with three energy carriers.

To deal with the high complexity of MES models, simplifications are sometimes necessary [8]. An example is the use of design days to make the model less complex. Instead of solving the model over a long time period (e.g. a full year), it is solved over smaller time periods of one or a few days that represent typical days (i.e.,

https://doi.org/10.52202/069564-0130

design days) of the year. [9] divide the year into 12 representative periods with a resolution of one hour, plus an extreme event, prior to the optimization. [10] represent the year using shiftable 24-hour periods.

There can also be simplifications in the mathematical model. Modeling an MES typically generates some non-linearities. Considering the difficulties in solving non-linear models, it can be more efficient to linearize the non-linear parts of a model to solve it using linear solvers. [11] linearizes the part-load efficiency of a combined heat and power unit (CHP) and optimizes the model over several typical 24-hour periods.

In this work, we aim to optimize a non-linear MES over a time period of one year with a temporal resolution of one hour. To do so, the system is first formulated as a non-linear mathematical programming model, which is then linearized using a set of auxiliary binary decision variables. Finally, the initial non-linear model is transformed into a mixed-integer linear programming (MILP) model. Solving the proposed MILP model for a period of one year with a temporal resolution of one hour is practically impossible using exact methods. Consequently, an innovative heuristic algorithm is proposed to solve the linearized model. Our proposed algorithm is significantly faster than commercial exact solvers (e.g., branch-and-bound) to solve the problem, while still obtaining good solutions very close to optimal ones.

The rest of this paper is organized as follows: Section 2. introduces the definition of the optimization problem and its mathematical formulation. Section 3. presents the proposed heuristic algorithm used to solve the problem. In Section 4. we employ the proposed algorithm to solve a real case study and compare the results of our algorithm with exact methods. Finally, Section 5. concludes the paper and provides further perspectives.

2. Problem definition

In this work, we study an MES with three energy carriers: electricity, heat, and gas, the latter being only used as fuel. The goal is to meet the energy demand of the system by optimizing the design and operation of the MES with a time resolution of one hour over a time horizon of one year.

The system is characterized by different generation technologies: a combined heat and power unit (CHP) to provide heat and electricity from gas using an internal combustion engine and a heat recovery system [12]; an electric boiler (EB) and a gas boiler (GB) to provide heat; two renewable energy sources (RES) that are photovoltaic (PV) panels to provide electricity and solar thermal (ST) panels to provide heat. The system can also interact with the grid to buy electricity or sell the surplus electricity produced by PV panels.

The system must provide energy to respond to the heat and electricity demands while optimizing two objectives: minimizing the cost of the system and maximizing the rate of RES. Therefore, the aim is to determine the design and operation of the MES while optimizing the two objectives and respecting the energy balance of the system.

2.1. Mathematical formulation

To perform the optimization, the MES is modeled as a mathematical program, shown in Equations (1a) to (1l). In this program and in the rest of this article, independent decision variables, which represent the optimal values to determine, are shown in bold (e.g. $\boldsymbol{P_{e,PV,t}}$). The other elements are parameters, i.e. fixed input data of the model.

$$\text{maximize} \quad ATCR = 100 * (1 - \frac{ATC_{MES}}{ATC_{ref}}) \tag{1a}$$

$$\tau_{RES} = 100 * \frac{\sum_{t\in\mathcal{T}}(\boldsymbol{P_{e,PV,t}} + \boldsymbol{P_{h,ST,t}})}{\sum_{t\in\mathcal{T}}(L_{e,t} + L_{h,t})} \tag{1b}$$

subject to

$$\boldsymbol{A_{PV}} + \boldsymbol{A_{ST}} \leq A_{total} \tag{1c}$$

$$\boldsymbol{P_{e,CHP,t}} \leq \boldsymbol{P_{CHP,nom}} \qquad \forall t \in \mathcal{T} \tag{1d}$$

$$\boldsymbol{P_{h,GB,t}} \leq \boldsymbol{P_{GB,nom}} \qquad \forall t \in \mathcal{T} \tag{1e}$$

$$\boldsymbol{P_{h,EB,t}} \leq \boldsymbol{P_{EB,nom}} \qquad \forall t \in \mathcal{T} \tag{1f}$$

$$\boldsymbol{P_{e,CHP,t}} = (a + b(\frac{\boldsymbol{P_{e,CHP,t}}}{\boldsymbol{P_{CHP,nom}}}) + c(\frac{\boldsymbol{P_{e,CHP,t}}}{\boldsymbol{P_{CHP,nom}}})^2)\boldsymbol{F_{g,CHP,t}} \qquad \forall t \in \mathcal{T} \tag{1g}$$

$$\boldsymbol{P_{h,CHP,t}} \leq \eta_{th,CHP}(\boldsymbol{F_{g,CHP,t}} - \boldsymbol{P_{e,CHP,t}}) \qquad \forall t \in \mathcal{T} \tag{1h}$$

$$\boldsymbol{V_{e,t}} + \boldsymbol{P_{e,PV,t}} = \boldsymbol{A_{PV}}\eta_{DC/AC}\eta_{ref}(1 - \alpha(30 + 0.0175(G_{\beta,t} - 300) + 1.14(T_{a,t} - 25) - T_{ref}))G_{\beta,t} \qquad \forall t \in \mathcal{T} \tag{1i}$$

$$\boldsymbol{P_{h,ST,t}} \leq \boldsymbol{A_{ST}}(G_{\beta,t}\eta_0 - U_{loss}(T_{w,m} - T_{a,t})) \qquad \forall t \in \mathcal{T} \tag{1j}$$

$$\boldsymbol{P_{e,CHP,t}} + \boldsymbol{P_{e,PV,t}} + \boldsymbol{U_{e,t}} - \frac{\boldsymbol{P_{h,EB,t}}}{\eta_{EB}} = L_{e,t} \qquad \forall t \in \mathcal{T} \tag{1k}$$

$$\boldsymbol{P_{h,CHP,t}} + \boldsymbol{P_{h,GB,t}} + \boldsymbol{P_{h,EB,t}} + \boldsymbol{P_{h,ST,t}} = L_{h,t} \qquad \forall t \in \mathcal{T} \tag{1l}$$

$$\boldsymbol{A_j} \in [A_j^{\min}, A_j^{\max}] \qquad \forall j \in \{PV, ST\} \tag{1m}$$

https://doi.org/10.52202/069564-0130

$$\boldsymbol{P_{j,nom}} \in [P^{\min}_{j,nom}, P^{\max}_{j,nom}] \qquad \forall j \in \{CHP, GB, EB\} \tag{1n}$$

$$\boldsymbol{P_{e,CHP,t}}, \boldsymbol{P_{h,CHP,t}}, \boldsymbol{F_{g,CHP,t}}, \boldsymbol{P_{h,GB,t}}, \boldsymbol{P_{e,PV,t}}, \boldsymbol{P_{h,ST,t}}, \boldsymbol{U_{e,t}}, \boldsymbol{V_{e,t}} \geq 0 \quad \forall t \in \mathcal{T} \tag{1o}$$

The first two formulas are the objective functions that are maximized: (1a) as the annual total cost reduction of the MES compared to a reference cost ATC_{ref}, and (1b) as the rate of RES used to respond to the energy demand. The annual total cost ATC_{MES} in (1a) is expressed as (2):

$$ATC_{MES} = \sum_{j \in \mathcal{M}} (C_{O\&M,j} + crf \cdot C_{inv,j}) - \sum_{t \in \mathcal{T}} I_{gr} \boldsymbol{V_{e,t}} + \sum_{t \in \mathcal{T}} (C_{gr,t} \boldsymbol{U_{e,t}} + C_g(\boldsymbol{F_{g,CHP,t}} + \tfrac{\boldsymbol{P_{h,GB,t}}}{\eta_{GB}})) \tag{2}$$

with $\mathcal{M} = \{CHP, GB, EB, PV, ST\}$ the set of technologies, $\mathcal{T} = (1, ..., 8760)$ the set of time steps of the year. I_g is the price of electricity sold, $\boldsymbol{V_{e,t}}$ the electricity sold at time t, $C_{gr,t}$ the cost of the electricity bought depending on the time of day t, $\boldsymbol{U_{e,t}}$ the electricity bought at time t, C_g the cost of gas bought, $\boldsymbol{F_{g,CHP,t}}$ the gas used by the CHP at time t, $\boldsymbol{P_{h,GB,t}}$ the heat of the GB at time t, and η_{GB} the efficiency of the GB.

The dependent variables $C_{O\&M,j}$ and $C_{inv,j}$ represent the operation and maintenance cost and the investment cost of each technology $j \in \mathcal{M}$, summarized in Table 1. *crf* is the capital recovery factor and represents the value of an annuity based on the number of annuities n and a discount factor i. It is expressed as $crf = i(1+i)^n/((1+i)^n - 1)$. Each technology j has an investment cost $\gamma_{inv,j}$, and an operation and maintenance cost with a fixed part $\gamma_{O\&M,j,f}$ and a variable part $\gamma_{O\&M,j,v}$. $P_{panel,nom}$ is the nominal power of a PV panel.

Table 1: Investment and operation costs of the technologies

Technology j	$C_{inv,j}$	$C_{O\&M,j}$
CHP	$\gamma_{inv,CHP} \boldsymbol{P_{CHP,nom}}$	$\gamma_{O\&M,CHP,v} \sum_{t \in \mathcal{T}} \boldsymbol{P_{e,CHP,t}}$
GB	$\gamma_{inv,GB} \boldsymbol{P_{GB,nom}}$	$\gamma_{O\&M,GB,f} \boldsymbol{P_{GB,nom}}$
EB	$\gamma_{inv,EB} \boldsymbol{P_{EB,nom}}$	$\gamma_{O\&M,EB,f} \boldsymbol{P_{EB,nom}} + \gamma_{O\&M,EB,v} \sum_{t \in \mathcal{T}} \boldsymbol{P_{h,EB,t}}$
PV	$\gamma_{inv,PV} P_{panel,nom} \boldsymbol{A_{PV}} / A_{panel}$	$\gamma_{O\&M,PV,f} P_{panel,nom} \boldsymbol{A_{PV}} / A_{panel}$
ST	$\gamma_{inv,ST} \boldsymbol{A_{ST}}$	$\gamma_{O\&M,ST,f} \boldsymbol{A_{ST}}$

The reference cost is calculated as the cost of responding to the demand using only the GB to generate heat and only buying electricity from the grid, calculated as (3):

$$ATC_{ref} = \gamma_{O\&M,GB,f} \max(L_{h,t}) + crf \cdot \gamma_{inv,GB} \cdot \max(L_{h,t}) + \sum_{t \in \mathcal{T}} (C_{gr,t} L_{e,t} + C_g \tfrac{L_{h,t}}{\eta_{GB}}) \tag{3}$$

The other equations and inequations in the model represent physical constraints. Equation (1c) constrains the maximum area of solar panels, with $\boldsymbol{A_{PV}}$ and $\boldsymbol{A_{ST}}$ the area of PV and ST panels and A_{total} the total area available for solar panels. (1d) to (1f) represent the limitation of the production by the installed capacity of the technologies with $P_{e,j,t}$ the electricity generated by technology j at time t, $P_{h,j,t}$ the heat generated by technology j at time t, and $P_{j,nom}$ the installed capacity of technology j. Equations (1g) and (1h) represent the power and heat production of the CHP. $\boldsymbol{F_{g,CHP,t}}$ is the gas consumption of the CHP, a, b, and c are the coefficients of electrical efficiency of the CHP, used by the function $a + b(\boldsymbol{P_{e,CHP,t}}/\boldsymbol{P_{CHP,nom}}) + c(\boldsymbol{P_{e,CHP,t}}/\boldsymbol{P_{CHP,nom}})^2$ that represents the electrical efficiency, depending on the part-load ratio of the CHP [12]. $\eta_{th,CHP}$ is the thermal efficiency of the CHP. Equation (1i) represents the electricity production from the PV panels. PV panels can sell the surplus produced power to the grid, represented by the variable $\boldsymbol{V_{e,t}}$. $\eta_{DC/AC}$ is the efficiency of PV inverters, η_{ref} is a reference efficiency for PV, α the temperature coefficient of the PV, $G_{\beta,t}$ the global solar radiation at time t, $T_{a,t}$ the ambient temperature at time t, and T_{ref} a reference temperature. (1j) is the production of heat from ST panels. η_0 is the optical efficiency of ST, U_{loss} the thermal loss coefficient, $T_{w,m}$ the mean water temperature in the ST collector. Equations (1k) and (1l) force the power and heat balance of the MES, with η_{EB} the efficiency of the EB, $L_{e,t}$ the electricity demand at time t, and $L_{h,t}$ the heat demand at time t. Finally, (1m), (1n), and (1o) represent the domain of the design and operation variables, respectively.

However, as seen in (1g), the CHP is governed by a non-linear efficiency function representing the part-load efficiency of the power generation of the CHP. Using a non-linear solver to solve a non-linear problem does not guarantee the optimality of the solution. We, therefore, propose to approximate this non-linear function by a piece-wise linear function to be able to model the system as a MILP.

2.2. Linearization

The efficiency function of the CHP in (1g) is linearized through a piece-wise linearization with two decision variables, adapted to the shape of the function. The proposed method of this paper is inspired by the so-called "triangle method" proposed by [13], which we adapt to the problem at hand. This type of method works by

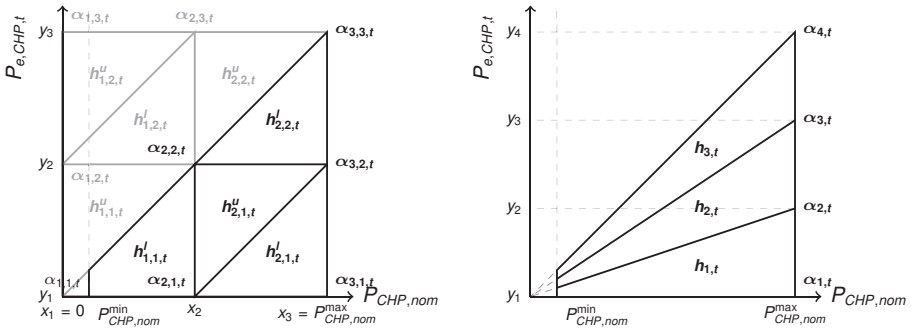

(a) "Triangle" method with $N = 3$ and $M = 3$ breakpoints (b) Adapted method with $N = 4$ breakpoints

Figure 1: Linearization methods examples

adding binary variables in the mathematical model to know which linear piece is selected. The mathematical program resulting from the addition of these binary variables is a MILP model, which can be solved by exact methods (e.g., branch-and-bound, branch-and-cut) [14], guaranteeing the optimality of the solution found.

The "triangle method" of [13] linearizes a function by introducing piece-wise linear parts in the form of triangles. However, in this work, half of those triangles are outside the feasible region of the problem. Figure 1a is an example of the application of the "triangle method". The x-axis is the variable $P_{CHP,nom}$, the y-axis the variable $P_{e,CHP,t}$, and the z-axis would be the function $F_{g,CHP,t}$ to linearize. $\alpha_{n,m,t}$ and $h_{n,m,t}$ represent the variables introduced in the model by this linearization method, N and M being the number of breakpoints on the x and y axes, respectively. As can be seen, half of the triangles are grayed out because they are outside the feasible region in our problem, enforced by Constraint (1d) of the model. This means that some variables and constraints would be added to the model without being useful in the present study. It also needs a large number of triangles to work with a small installed capacity of the CHP for this problem. Looking again at Fig 1a, for the linearization to be effective, the value of $\boldsymbol{P_{CHP,nom}}$ must be greater than x_2, otherwise it would be equivalent to a linearization with a single triangle. Furthermore, a MILP model, with binary or integer variables, while being able to be solved to optimality, is still harder to solve than a linear program (LP) with only continuous variables. Accordingly, reducing the number of binary variables can greatly reduce the complexity of the problem.

We therefore propose an "adapted" version of the triangle method to use fewer triangles and ignore the area outside the feasible region. The adapted method better follows the function we are looking to linearize and uses fewer binary variables, and it is not subject to the inaccurate linearization mentioned for the triangle method when there is a small installed capacity. It introduces continuous variables, noted $\boldsymbol{\alpha_{n,t}} \in [0,1],\ \forall n \in \{1,...,N\}, t \in \mathcal{T}$, and binary variables, noted $\boldsymbol{h_{n,t}} \in \{0,1\},\ \forall n \in \{1,...,N-1\}, t \in \mathcal{T}$, for each breakpoint $n \in \{1,...,N\}$ in the linearization and at each time step $t \in \mathcal{T}$. N is a parameter of the linearization and is the number of breakpoints introduced (and therefore $N-1$ is the number of triangles). We choose to linearize the function $F_{g,CHP,t}$ written as (4).

$$F_{g,CHP,t} = \frac{P_{e,CHP,t}}{a + b\frac{P_{e,CHP,t}}{P_{CHP,nom}} + c(\frac{P_{e,CHP,t}}{P_{CHP,nom}})^2} \tag{4}$$

We need the value of this function at different breakpoints over $P_{e,CHP,t}$, noted $y_n = P^{max}_{CHP,nom} \times (n-1)/(N-1)$:

$$f(y_n) = \frac{y_n}{a + b\frac{y_n}{P^{max}_{CHP,nom}} + c(\frac{y_n}{P^{max}_{CHP,nom}})^2} \tag{5}$$

Equations (6a) to (6f) represent the linearization constraints used to replace (1g). We consider N breakpoints, and a convex combination of the values $\boldsymbol{\alpha_{n,t}}$ can approximate the values of the linearized variables $\boldsymbol{P_{CHP,nom}}$, $\boldsymbol{P_{e,CHP,t}}$, and $\boldsymbol{F_{g,CHP,t}}$. Equation (6e) ensures that only one triangle h is selected at each time step, and (6f) ensures that only the coefficients α associated with the selected triangle have non-zero values, with dummy values $h_{0,t} = 0$ and $h_{N,t} = 0$. (6g) and (6h) constrain the domain of the linearization variables. An example with

https://doi.org/10.52202/069564-0130

N = 4 breakpoints is presented in Fig 1b.

$$\sum_{n=1}^{N} \boldsymbol{\alpha_{n,t}} \leq 1 \qquad \forall t \in \mathcal{T} \tag{6a}$$

$$\boldsymbol{P_{CHP,nom}} = \sum_{n=1}^{N} \boldsymbol{\alpha_{n,t}} P^{\max}_{CHP,nom} \qquad \forall t \in \mathcal{T} \tag{6b}$$

$$\boldsymbol{P_{e,CHP,t}} = \sum_{n=1}^{N} \boldsymbol{\alpha_{n,t}} y_n \qquad \forall t \in \mathcal{T} \tag{6c}$$

$$\boldsymbol{F_{g,CHP,t}} = \sum_{n=1}^{N} \boldsymbol{\alpha_{n,t}} f(y_n) \qquad \forall t \in \mathcal{T} \tag{6d}$$

$$\sum_{n=1}^{N-1} \boldsymbol{h_{n,t}} = 1 \qquad \forall t \in \mathcal{T} \tag{6e}$$

$$\boldsymbol{\alpha_{n,t}} \leq \boldsymbol{h_{n,t}} + \boldsymbol{h_{n-1,t}} \qquad \forall n \in \{1, ..., N\}, t \in \mathcal{T} \tag{6f}$$

$$\boldsymbol{\alpha_{n,t}} \in [0, 1] \qquad \forall n \in \{1, ..., N\}, t \in \mathcal{T} \tag{6g}$$

$$\boldsymbol{h_{n,t}} \in \{0, 1\} \qquad \forall n \in \{1, ..., N-1\}, t \in \mathcal{T} \tag{6h}$$

The problem is studied through a multi-objective perspective, optimizing both the cost of the MES and the rate of RES producing energy. It is not possible to improve both objectives at the same time, since the improvement of one objective implies a degradation of another one. Therefore, we calculate a set of non-dominated solutions on the so-called Pareto front. The ϵ-constraint method [15] is used to calculate a set of solutions on the Pareto front, from which the decision maker can choose the solution that best corresponds to his or her preferences, as a trade-off between the two objective functions. This method works by maximizing one objective function while setting a constraint on the other objective function. Modifying the value of this constraint allows us to obtain several optimal solutions.

Although linearizing the non-linear model makes it computationally easier to be solved, solving the proposed MILP model is still challenging. The binary variables introduced to the model make it combinatorial and NP-hard to solve. It is possible to obtain optimal solutions for shorter time horizons, up to a few weeks, but the resolution of the model over the time horizon of one year is intractable in a reasonable computation time.

In this work, our goal is therefore to improve the resolution time of this model while obtaining good quality solutions. To this end, we propose in the next section a heuristic to solve the problem over long time horizons while maintaining good-quality solutions.

3. Solution approach

We propose a heuristic algorithm to reduce the complexity of the model by letting the binary variables be continuous while guaranteeing the binary value of these variables. Heuristics are approximate algorithms that aim to provide good solutions to a specific problem in a limited computation time [16]. They do not guarantee the optimality of the solution, but are generally faster than exact methods.

The proposed heuristic is composed of two subsequent steps: 1) Initialization and 2) Iterative local search. The initialization generates an initial solution by relaxing the binary variables of the proposed MILP model, and the local search aims to iteratively improve the generated initial solution toward the optimal solution.

These two high-level steps are summarized in Algorithm 1. First, the MILP model is generated with the set of parameters $\mathcal{P}$ of the case study (line 2). A relaxed MILP model, detailed in Section 3.1., is then created from the MILP (line 3), and an initial solution is found after solving this model (line 4). Second, a local search, described in Section 3.2., is used iteratively on the initial solution until there is no improvement. The values of the objective functions are compared to their best values so far (line 5 of Algorithm 1), and if the new solution is better, the next iteration of the local search starts.

As there are two objective functions *ATCR* and τ_{RES} in the model, subscripts 1 and 2 indicate the first and second objective functions, respectively. In the proposed heuristic algorithm, the vector ($bestObj_1$, $bestObj_2$) represents the best value of the objective functions found so far, and (obj_1, obj_2) is the vector of the objective functions of the current solution. We consider that the solution *a* is better than the solution *b* if the first objective function of *a* is better, or if the second objective function of *a* is better and the first objective function of *a* is at least as good. As an example, consider *ATCR* and τ_{RES} as the first and second objective functions, respectively. Solution *a* is better than *b* if $ATCR^a > ATCR^b$, or $\tau^a_{RES} > \tau^b_{RES}$ and $ATCR^a \geq ATCR^b$.

3.1. Initialization

As the first step of the heuristic algorithm, a relaxation method is used to generate an initial solution to the problem: the binary variables that allow knowing which triangle is selected at each time step are relaxed to be continuous (i.e., have a value between zero and one), transforming the MILP model into an LP model which is much easier to solve by using, for example, the Simplex class of algorithms. All other variables and constraints remain unchanged. The relaxed MILP model is solved as a linear model and, therefore, the continuous relaxed variables $\boldsymbol{h_{n,t}}$ have a value in [0, 1].

This process is explained in Algorithm 2. The first relaxed MILP model is solved on line 2. Then, at each time

Algorithm 1 High-level algorithm

1: $(bestObj_1, bestObj_2) \leftarrow (-\infty, -\infty)$
2: $MILP \leftarrow$ GENERATEMILP($\mathcal{P}$)
3: $relaxedMILP \leftarrow$ RELAX($MILP$)
4: $(obj_1, obj_2),\ sol \leftarrow$ CREATEINITIALSOLUTION($relaxedMILP$) ▷ Find initial solution
5: **while** $obj_1 > bestObj_1$ or $obj_1 \geq bestObj_1$ and $obj_2 > bestObj_2$ **do**
6: $\quad (bestObj_1, bestObj_2),\ bestSol \leftarrow (obj_1, obj_2),\ sol$
7: $\quad (obj_1, obj_2),\ sol \leftarrow$ LOCALSEARCH($relaxedMILP$, $bestSol$) ▷ Improve the solution
8: **end while**
9: **return** $bestSol$

step $t \in \mathcal{T}$, the variable with the highest value among $\boldsymbol{h_{1,t}}, ..., \boldsymbol{h_{N-1,t}}$ is selected, and a constraint is added to the model to force this variable to be equal to 1, on line 3 of the algorithm. The relaxed MILP model is again solved with these additional constraints on line 4, obtaining this time a feasible solution with all the relaxed variables $\boldsymbol{h_{n,t}}$ having a value of 0 or 1, which gives us the initial solution for the heuristic.

In these algorithms, $\mathcal{N}$ is the ordered set of the triangle indices: $\mathcal{N} = (1, ..., N-1)$. H is the set of variables representing the triangles selected: $H = \{\boldsymbol{h_{n,t}},\ \forall n \in \mathcal{N}, t \in \mathcal{T}\}$. They have binary values in the MILP model or real values in the relaxed MILP model. sol is a vector of the index n of the triangle selected at each time step, i.e. $sol = (\{n : \boldsymbol{h_{n,t}} = 1, \forall n \in \mathcal{N}\},\ \forall t \in \mathcal{T})$ if the variables are binary.

Algorithm 2 Initial solution search algorithm

1: **function** CREATEINITIALSOLUTION($relaxedMILP$)
2: $\quad (obj_1, obj_2),\ H \leftarrow$ SOLVE($relaxedMILP$) ▷ Solve relaxed MILP
3: $\quad H_N^{\max} \leftarrow (\arg\max_n(\boldsymbol{h_{n,t}}),\ \forall t \in \mathcal{T})$ ▷ Get the max. argument n for each time step
4: $\quad C \leftarrow \{\boldsymbol{h_{n,t}} = 1,\ \forall n \in H_N^{\max}, t \in \mathcal{T}\}$ ▷ Construct set of constraints to force a triangle to 1 at each time step
5: $\quad (obj_1, obj_2),\ H \leftarrow$ SOLVE($relaxedMILP \cup C$) ▷ Solve relaxed MILP with additional constraints C
6: $\quad sol \leftarrow (\{n : \boldsymbol{h_{n,t}} = 1, \forall n \in \mathcal{N}\},\ \forall t \in \mathcal{T})$ ▷ Get vector of arguments n where $\boldsymbol{h_{n,t}} = 1$ for each time step
7: $\quad$ **return** $(obj_1, obj_2),\ sol$
8: **end function**

3.2. Local search

The second step is to improve the initial solution found. For this aim, we developed a local search method to improve the initial solution by looking at its neighborhood. A local search method works by applying small local changes to a solution with the aim of improving the solution and is applied iteratively until a stopping criterion is reached, e.g. the solution does not improve further, or a time limit fixed in advance is exceeded.

In this work, the local search starts from the initial solution found previously using Algorithm 2. Adjacent linearization triangles of this initial solution are selected to obtain a better solution. For example, in Fig 1b, we can see that if $\boldsymbol{h_{1,t}} = 1$, the first triangle is selected, and if $\boldsymbol{\alpha_{2,t}} > 0$ and $\boldsymbol{\alpha_{1,t}} = 0$, that would mean that the point selected is on the edge between the first and second triangle, and we could choose to select the second triangle without degrading the solution.

Using this knowledge, our local search method selects the other triangle each time a value of the linearization is on the edge of a triangle, executed on lines 2 to 9 of Algorithm 3. For each time step $t \in \mathcal{T}$, for each triangle n selected, if the value of $\alpha_{n,t} = 0$ we select the next triangle, and otherwise if the value of $\alpha_{n+1,t} = 0$ we select the previous triangle. If no value $\alpha_{n,t}$ or $\alpha_{n+1,t}$ is null, we are not on the edge of the triangle and therefore keep the same triangle selected. The selected triangles become constraints in the linear program, i.e. a constraint $h_{n,t} = 1$ is added for the triangle n selected at time step t, $\forall t \in \mathcal{T}$. The linear model is again solved with the newly selected triangles. The new constraints to force the selected triangles are created on line 10, the relaxed MILP model is solved with these constraints on line 11, and the new solution is then constructed on line 12.

A new iteration of the local search is started if the new solution is better than the previous one. Otherwise, the algorithm stops and the best solution found is considered as the solution of the algorithm.

4. Case study

4.1. Description

An instance of the problem defined in Section 2. is used to compare the solutions of the heuristic algorithm and the MILP resolution with real-world data. The MES studied in the present case study covers an area of 33.5 hectares in the vicinity of Nantes, France. It includes the campus of IMT Atlantique, a French technological university, and 45 single-family houses. There are two objective functions to optimize: the maximization of the cost reduction of the MES (i.e. the minimization of the cost of the MES compared to a reference cost), and the maximization of the rate or RES used to respond to the energy demand. The values of the parameters of the

https://doi.org/10.52202/069564-0130

Algorithm 3 Local search algorithm

function LOCALSEARCH(*relaxedMILP*, *sol*)
  for all $t \in \mathcal{T}$ **do**
    $n \leftarrow sol_t$ ▷ Index n of triangle selected for time t
    if $\alpha_{n,t} = 0$ and $n < N - 1$ **then**
      $sol_t \leftarrow sol_t + 1$
    else if $\alpha_{n+1,t} = 0$ and $n + 1 > 1$ **then**
      $sol_t \leftarrow sol_t - 1$
    end if
  end for
  $C \leftarrow \{\boldsymbol{h}_{\boldsymbol{sol_t,t}} = 1,\ \forall t \in \mathcal{T}\}$ ▷ Construct set of constraints for the new triangles
  $newObj,\ H \leftarrow$ SOLVE($relaxedMILP \cup C$) ▷ Solve relaxed MILP with selected triangles *sol*
  $newSol \leftarrow (\{n : \boldsymbol{h}_{\boldsymbol{n,t}} = 1, \forall n \in \mathcal{N}\},\ \forall t \in \mathcal{T})$
  return *newObj*, *newSol*
end function

model for this case study are summarized in Tables 2 and 3. The energy demands, the temperature, and the global solar radiation over the year are time series parameters.

Table 2: Cost (investment and operation) parameters per technology

Technology j	$\gamma_{inv,j}$	$\gamma_{O\&M,j,f}$	$\gamma_{O\&M,j,v}$
CHP	1140 €/kW	-	21 €/MWh
GB	90 €/kW	3.15 €/(kW year)	-
EB	100 €/kW	1 €/(kW year)	0.8 €/MWh
PV	1000 €/kW	15 €/(kW year)	-
ST	615 €/m^2	10 €/(m^2 year)	-

4.2. Methodology

The model is solved using an MILP solver and the proposed heuristic algorithm to compare the two resolution methods. Three periods of the year of one week are studied: one week in winter when there is high demand variability and low RES generation, one week in summer when there are lower demands and high RES potential, and one week in mid-season when the demand is lower but there is still a high RES potential.

The time horizon of one week allows us to obtain the optimal solution for the MILP model, and therefore, by comparison, to evaluate the quality of the output of the proposed heuristic algorithm. For each of the three periods, 10 solutions are calculated on the Pareto front using the ϵ-constraint method explained in Section 2., with solution 1 being the solution with the most RES and solution 10 the solution with the highest cost reduction. The number of breakpoints for the linearization was set by trial and error at a value $N = 10$ (i.e. $N - 1 = 9$ triangles), giving a good trade-off between the precision of the linearization and the complexity of the model.

The two methods are compared in terms of the quality of the solution using a *Mean Ideal Distance* indicator to compare the Pareto fronts obtained. This indicator compares the solutions of the two Pareto fronts, as the mean difference of the distance of each solution to an ideal point at the origin, as detailed in (7), with $\mathcal{S} = \{1, ..., 10\}$ the 10 solutions calculated.

$$mean\ distance = \frac{1}{|\mathcal{S}|} \sum_{s \in \mathcal{S}} \left(\sqrt{ATCR_s^{optimal^2} + \tau_{RES_s}^{optimal^2}} - \sqrt{ATCR_s^{heuristic^2} + \tau_{RES_s}^{heuristic^2}} \right) \tag{7}$$

An error indicator also allows us to compare the result of the heuristic algorithm with the optimal solution, by calculating the error between the heuristic solution and the MILP solution for the two objective functions and the $|\mathcal{S}|$ solutions, as in (8).

$$error = \left\{ \left| \frac{f_s^{optimal} - f_s^{heuristic}}{f_s^{optimal}} \right|, \quad \forall f \in \{ATCR, \tau_{RES}\}, s \in \mathcal{S} \right\} \tag{8}$$

The maximum, mean, and standard deviation are calculated and shown in the table.

The solutions are also compared in terms of the total computation time for the $|\mathcal{S}|$ solutions.

An energy analysis is also performed to compare the two methods. The difference between the values of the operation variables for the two variables is presented at each time step, in the form of a boxplot. As an example, the set $v = \{P_{e,CHP,t}^{heuristic} - P_{e,CHP,t}^{optimal},\ \forall t \in \mathcal{T}\}$ would be presented as a boxplot for the electricity produced by the CHP. Whiskers are represented to show the 5th and 95th percentiles of each set. These figures are

Table 3: General parameters of the case study

$P^{min}_{CHP,nom}$ = 100 kW, $P^{max}_{CHP,nom}$ = 1000 kW	Minimum and maximum nominal power of the CHP
$P^{min}_{GB,nom}$ = 100 kW, $P^{max}_{GB,nom}$ = 3000 kW	Minimum and maximum nominal power of the GB
$P^{min}_{EB,nom}$ = 100 kW, $P^{max}_{EB,nom}$ = 3000 kW	Minimum and maximum nominal power of the EB
A^{min}_{PV} = 0 m^2, A^{max}_{PV} = 10 000 m^2	Minimum and maximum area of the PV panels
A^{min}_{ST} = 0 m^2, A^{max}_{ST} = 10 000 m^2	Minimum and maximum area of the ST panels
$L_{e,t}$ (kW)	Electricity demand of the system
$L_{h,t}$ (kW)	Heat demand of the system
a = 0.1, b = 0.4, c = -0.2	Electrical efficiency coefficients of the CHP
β = 0.3	Constant CHP electrical efficiency
$\eta_{th,CHP}$ = 0.8	Thermal efficiency of the heat recuperation system of the CHP
η_{GB} = 0.8	Efficiency of the GB
η_{EB} = 0.8	Efficiency of the EB
$\eta_{DC/AC}$ = 0.9	PV inverters' efficiency
η_{ref} = 0.155	Reference efficiency for PV
$G_{\beta,t}$ (W m^{-2})	Global solar radiation
α = 0.43 %/°C	Temperature coefficient of PV
T_{ref} = 25 °C	Reference temperature
$T_{a,t}$ (°C)	Outdoor temperature
$P_{panel,nom}$ = 250 W	Nominal power of a PV panel
A_{panel} = 1.6 m^2	Area of a PV panel
η_0 = 0.8	Optical efficiency of ST
U_{loss} = 5 W m^{-2} °C^{-1}	Thermal loss coefficient of ST
$T_{w,m}$ = 45 °C	Mean water temperature in the ST collector
A_{total} = 10 000 m^2	Total area available for solar panels
$C_{gr,t}$ = 0.13 €/kWh	Cost of electricity bought from the grid (0h–7h)
$C_{gr,t}$ = 0.17 €/kWh	Cost of electricity bought from the grid (8h–23h)
C_g = 0.076 €/kWh	Cost of gas bought
I_{gr} = 0.1 €/kWh	Price of electricity sold to the grid

presented for each of the three one-week periods, each time for the $|\mathcal{S}| = 10$ solutions of the Pareto set. These figures will show the difference in the MILP and heuristic solutions from an operation standpoint by highlighting the difference in the power generated by the different technologies.

An energetic analysis will also be presented, with the energy balance of each technology being calculated for the worst solution of each season. Energy is calculated as the integral of the power generated by each technology over the time period, e.g. $E_{e,CHP} = \sum_{t\in\mathcal{T}} P_{e,CHP,t}$ for the electric energy balance of the CHP.

Capacity factors are also presented, showing the difference in the usage of each technology between the MILP and heuristic solutions. It is the ratio of the energy output of a technology over the maximum theoretical energy output based on the installed capacity. As an example for the GB, it is calculated as (9):

$$\mathrm{CF}_{GB} = 100 \times \frac{\sum_{t\in\mathcal{T}} \boldsymbol{P_{h,GB,t}}}{|\mathcal{T}|\boldsymbol{P_{GB,nom}}} \tag{9}$$

For the RES the maximum theoretical energy depends on the environmental conditions, as in 10 for the ST:

$$\mathrm{CF}_{ST} = 100 \times \frac{\sum_{t\in\mathcal{T}} \boldsymbol{P_{h,ST,t}}}{\sum_{t\in\mathcal{T}} \boldsymbol{A_{ST}}(G_{\beta,t}\eta_0 - U_{loss}(T_{w,m} - T_{a,t}))} \tag{10}$$

The installed capacity of the CHP is expressed in its electrical installed capacity, so the maximum theoretical heat energy is calculated using $\eta_{e,CHP} = 0.3$, which is the best theoretical electrical efficiency given the values of the parameters a, b, and c, which gives a capacity factor for the heat of the CHP calculated as (11):

$$\mathrm{CF}_{h,CHP} = 100 \times \frac{\sum_{t\in\mathcal{T}} \boldsymbol{P_{h,CHP,t}}}{|\mathcal{T}|\boldsymbol{P_{CHP,nom}}\eta_{th,CHP}(1 - 0.3)} \tag{11}$$

Finally, a resolution of the model is performed over the full year using the proposed heuristic algorithm. The computation time is compared with the resolution of the full year using a MILP solver with an optimality gap as a stop criterion, to have an idea of the time required to solve the full year to optimality.

4.3. Results

The optimal solutions are obtained using the Gurobi solver (version 9.5.2), and the heuristic was implemented in Python with the same version of Gurobi used to solve the relaxed MILP. All the solutions were computed

https://doi.org/10.52202/069564-0130

on a computation server with 400GB RAM and Intel Xeon Gold 6138 @ 2.00GHz CPUs, using 32 threads for Gurobi and one thread in Python.

Table 4 shows the computation times of the two methods for the three different periods (winter, summer, and mid-season). The optimal time and the heuristic time are the total time necessary to obtain the 10 solutions for each method and each period. The improvement is the relative difference between the two durations.

Table 4: Comparison of the total computation time over 3 one-week periods

Period	Optimal time	Heuristic time	Improvement
Winter	1182.4 s	4.1 s	99.7 %
Summer	42.3 s	1.1 s	97.4 %
Mid-season	1802.0 s	2.0 s	99.9 %

As can be seen for the mid-season period, the MILP solver can take a really long time to find the solution. This period is especially complex because it is the season where the energy demand varies the most from day to day, but there is still enough solar radiation to make the RES a good option to generate energy. On average, for the three periods computed here, the heuristic algorithm is 99.0 % faster than the MILP solver.

Table 5 shows the error of the heuristic method compared to the optimal solutions found when solving the MILP model, i.e. the maximum, mean, and standard deviation of the errors calculated from (8). It also shows how many times the heuristic algorithm found the optimal solution.

Table 5: Precision of the heuristic algorithm

Period	Error			Nbr. optimal solutions
	Max.	Mean	SD	(out of 10)
Winter	6.6×10^{-5}	6.8×10^{-6}	1.6×10^{-5}	4
Summer	2.5×10^{-15}	7.2×10^{-16}	6.9×10^{-16}	6
Mid-season	3.1×10^{-10}	1.6×10^{-11}	7.0×10^{-11}	4

We can see that the heuristic obtains good solutions, the maximum error being 6.6×10^{-5} and the average mean error 2.3×10^{-6}. Furthermore, the heuristic found the optimal solution 14 times out of the 30 solutions computed.

This shows that the heuristic method works well for small time periods, giving good-quality solutions with a much smaller computation time than the MILP.

Figure 2 presents boxplots of the difference between the values of the operation variables of the MILP and the heuristic resolutions. The x-axis of each subplot represents the 10 solutions of the Pareto front, and the y-axis is the difference in the operation's variables. When there is no symbol for ST, that means that no ST panels are installed for this solution. We can see that the ST panels are installed only in winter and on the first solutions, when we focus on maximizing the RES. In these boxplots, the whiskers represent the 5th and 95th percentiles, and the points are the outliers outside this range. As can be seen in the figure, the "box" is never visible, meaning that the first and third quartiles always coincide with the median; therefore, at least 50 % of the operation variables of each technology are identical between the solutions of the MILP and of the heuristic. Most of the time, the 5th and 95th percentile whiskers also coincide with the median, meaning that more than 90 % of the solutions are the same. The difference is larger in winter and smaller in summer. This can be explained because the energy demands have a larger variability with a greater maximum demand in winter.

Another analysis that can be drawn from Fig 2 is that the two resolution methods can have different operation plans but still be optimal in terms of the mathematical program. During the winter week, for solutions 2, 3, 4, and 5 the MILP solver and the heuristic give the same values for the two objective functions, the same installed capacities, and the same triangles selected for the linearization. However, solutions 2, 3, and 4 on the boxplots 2a show that the operation variables are slightly different. The same is true for the summer week, with solutions 1, 2, 3, 4, 5, and 10 being optimal but having different values for the operation variables for solutions 2, 3, 4, and 5 on 2b, and for the mid-season week, with solutions 1, 2, 3, and 10 being optimal but solutions 2 and 3 having different operation values on 2c. This can happen because the energy balance is identical, but the energy might be used at different times of the week.

It can also be observed that ST panels are not installed during the summer and mid-season weeks, and ST panels appear in winter only when there is a high value for the objective function τ_{RES}.

Table 6 presents the energy balance of the solution with the largest difference between the MILP and the heuristic solution for each time period. The underlined cells show the technologies with a difference between the two solutions. The relative differences in the values of the objectives functions for these solutions are

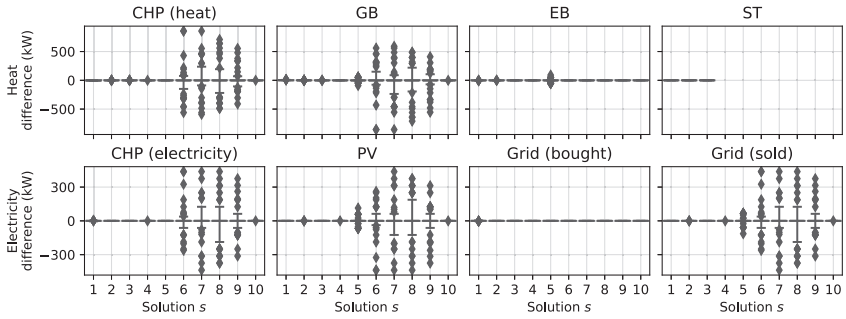

(a) 1 week in winter

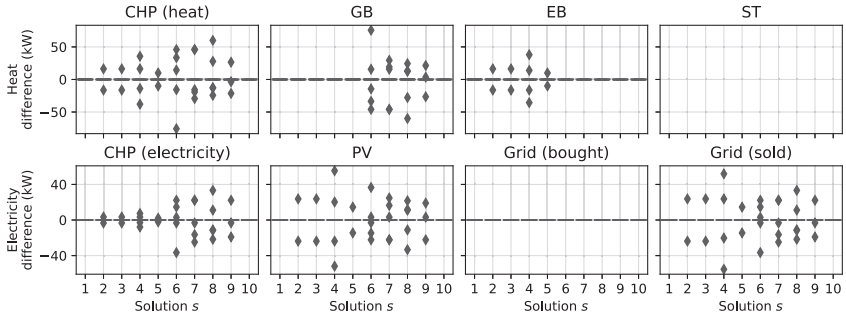

(b) 1 week in summer

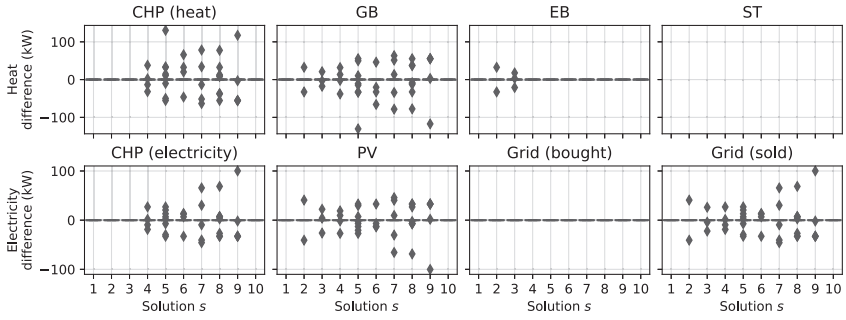

(c) 1 week in mid-season

Figure 2: Difference in the operation of the MILP and heuristic resolutions

6.6×10^{-3} %, 1.6×10^{-13} %, and 3.1×10^{-8} % for *ATCR*, and 0 %, 3.3×10^{-14} %, and 1.9×10^{-14} % for τ_{RES}, for the winter, summer, and mid-season week presented, respectively. As can be seen, the difference is small even in the worst cases. For the summer and mid-season solutions, only the heat produced by the CHP and the GB are different between the MILP and the heuristic solution, with the CHP heat energy being slightly higher for the heuristic and the GB energy slightly lower. For the winter week, the energy produced by the EB is also different, and there is also a difference in the electrical energy produced by the CHP and the electricity imported from the grid.

Table 7 presents the capacity factors, calculated using (9), (10), and (11), for the same selected solutions. For these solutions, the installed capacity is the same for the summer and mid-season solutions. The installed capacity is different for some of the technologies for the winter week, with the largest difference being only 11 kW for the GB or a relative difference of 0.8 %. The capacity factor is also very similar, the largest difference being 0.4 % for the electrical capacity factor of the CHP for the winter solution.

As an example, Fig 3 shows the operation of the 8th solution of the winter week for the MILP model and the heuristic algorithm. As can be seen in the figure, the operation can be different at certain time steps. However, the values of the objective functions are very similar, with a relative difference of 6.9×10^{-6} % for *ATCR* and 8.4×10^{-4} % for τ_{RES}. This can be explained by the fact that the operation variables intervene always as the sum of the variables over the time period considered, i.e. as the energy over the time period. Two solutions can be very similar in terms of energy but have different operation plans to reach the same energy. In other words,

https://doi.org/10.52202/069564-0130

Table 6: Energy balance of the most different solutions

Technology	Winter, solution 1 MILP	Winter, solution 1 Heuristic	Summer, solution 7 MILP	Summer, solution 7 Heuristic	Mid-season, solution 5 MILP	Mid-season, solution 5 Heuristic
CHP (heat)	135.65 MWh	135.21 MWh	8.89 MWh	8.92 MWh	46.27 MWh	46.38 MWh
GB	84.78 MWh	85.25 MWh	273.60 kWh	246.06 kWh	18.32 MWh	18.22 MWh
EB	261.66 kWh	245.40 kWh	0.00 Wh	0.00 Wh	132.62 kWh	132.62 kWh
ST	24.47 MWh	24.47 MWh	0.00 Wh	0.00 Wh	0.00 Wh	0.00 Wh
CHP (elec)	69.10 MWh	68.97 MWh	3.58 MWh	3.58 MWh	23.60 MWh	23.60 MWh
PV	16.51 MWh	16.51 MWh	27.01 MWh	27.01 MWh	22.62 MWh	22.62 MWh
Grid (bought)	3.00 MWh	3.11 MWh	23.48 MWh	23.48 MWh	8.63 MWh	8.63 MWh

Table 7: Capacity factors of the most different solutions

	Winter, solution 1				Summer, solution 7				Mid-season, solution 5			
	MILP		Heuristic		MILP		Heuristic		MILP		Heuristic	
Technology	Factor	Capacity	Factor	Capacity	Factor	Capacity	Factor	Capacity	Factor	Capacity	Factor	Capacity
CHP (heat)	82.0 %	–	82.3 %	–	29.6 %	–	29.7 %	–	52.2 %	–	52.4 %	–
GB	36.2 %	1395 kW	36.1 %	1406 kW	1.6 %	100 kW	1.5 %	100 kW	22.4 %	486 kW	22.3 %	486 kW
EB	1.6 %	100 kW	1.5 %	100 kW	0.0 %	100 kW	0.0 %	100 kW	0.8 %	100 kW	0.8 %	100 kW
CHP (elec)	74.6 %	552 kW	75.0 %	547 kW	21.3 %	100 kW	21.3 %	100 kW	47.6 %	295 kW	47.6 %	295 kW
ST	67.9 %	4756 m^2	67.9 %	4756 m^2	–	0 m^2	–	0 m^2	–	0 m^2	–	0 m^2
PV	100.0 %	5244 m^2	100.0 %	5244 m^2	63.6 %	10 000 m^2	63.6 %	10 000 m^2	58.8 %	10 000 m^2	58.8 %	10 000 m^2

the technologies produce almost the same energy at different time steps over the time period. However, the difference is acceptable in the objective of optimal design taking into account the operation (control aspects being out of the scope of this work).

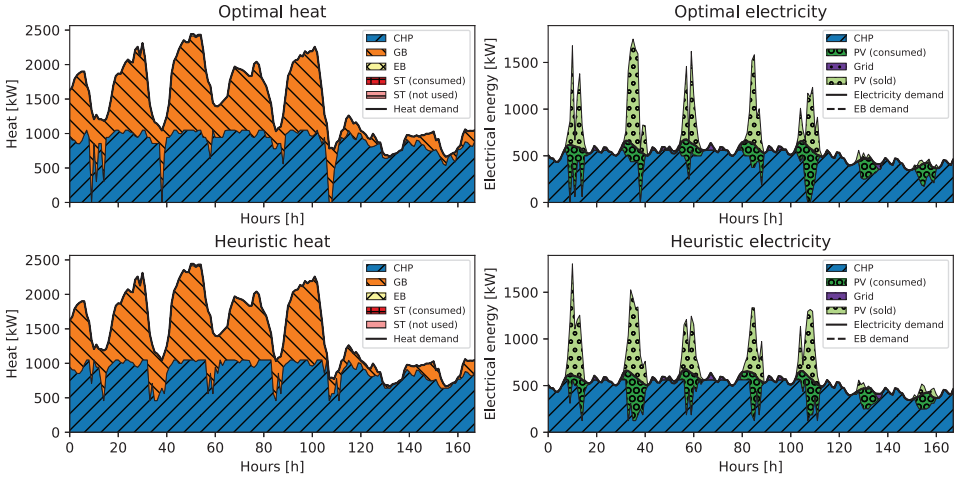

Figure 3: Operation for a MILP and heuristic solution (winter week, solution 8)

Finally, the model was solved with the heuristic algorithm for the full time period of one year, and a MILP solver was used to try to solve the same model for the entire year. The solver was stopped when its optimality gap reached 0.1 %, as it is not possible to obtain an optimal solution in a reasonable time.

The heuristic algorithm took 549.9 s to find results for the 10 solutions of the Pareto front. The MILP solver took 5.6×10^5 s, or 156.7 h to find the 10 solutions. That represents an improvement of 99.9 %. The average relative differences for the 10 solutions of the Pareto front are 1.1 % and -1.7 % for *ATCR* and τ_{RES}, respectively, with the heuristic giving better solutions than the MILP solver for *ATCR*. However the MILP solver was stopped before obtaining an optimal solution.

5. Conclusion and perspectives

This paper presented the modeling of an MES as a non-linear mathematical programming model. A piece-wise linearization method was used to linearize the model and obtain a MILP model. However, it has been shown that the computation time can be intractable for optimizing the MILP model over a long time period of one year. Consequently, a heuristic algorithm was proposed to solve the MILP model. The proposed algorithm finds an

initial solution through a relaxed MILP model, then uses a local search to iteratively improve the initial solution by finding which piece of the linearization to select.

A comparison of the resolution of small time periods of one week of the model through a MILP solver and through the heuristic algorithm showed that the heuristic is capable of finding solutions close to the optimum. It has also been shown that different operations of the MES can be optimal with regard to the mathematical program. Even when the solution found by the heuristic is not optimal, the capacity factors of the different technologies are close to the optimum values. The heuristic algorithm was shown to be faster than the resolution using a MILP solver, with an improvement of more than 99.9 % when solving a long time period of a year.

Although the proposed heuristic algorithm is very fast on the MES model presented in this article, further experimentation on other linearized models is still needed to determine if this method is generalizable for solving other problems. Additional work is also needed to evaluate the robustness of the initialization method and the local search, as relaxation of the MILP model could theoretically lead to infeasible solutions. Further experiments should also be conducted to compare the solutions of the heuristic algorithm and the MILP resolution over the full year, to assess whether the heuristic is still efficient when solving long time periods.

References

[1] Geidl M. et al. *Energy hubs for the future*. In: "IEEE Power and Energy Magazine" 5.1 (Jan. 2007), pp. 24–30. DOI: 10.1109/mpae.2007.264850.

[2] Fabrizio E., Filippi M., and Virgone J. *Trade-off between environmental and economic objectives in the optimization of multi-energy systems*. In: "Building Simulation" 2.1 (Mar. 2009), pp. 29–40. DOI: 10.1007/s12273-009-9202-4.

[3] Frangopoulos C. A., Spakovsky M. R. von, and Sciubba E. *A Brief Review of Methods for the Design and Synthesis Optimization of Energy Systems*. In: "International Journal of Applied Thermodynamics" 5.4 (Dec. 2002), pp. 151–160. ISSN: 1301-9724. DOI: 10.5541/ijot.97.

[4] Wirtz M. et al. *Design optimization of multi-energy systems using mixed-integer linear programming: Which model complexity and level of detail is sufficient?* In: "Energy Conversion and Management" 240 (July 2021), p. 114249. ISSN: 0196-8904. DOI: 10.1016/j.enconman.2021.114249.

[5] Poncelet K. et al. *Impact of the level of temporal and operational detail in energy-system planning models*. In: "Applied Energy" 162 (Jan. 2016), pp. 631–643. DOI: 10.1016/j.apenergy.2015.10.100.

[6] Klemm C. and Vennemann P. *Modeling and optimization of multi-energy systems in mixed-use districts: A review of existing methods and approaches*. In: "Renewable and Sustainable Energy Reviews" 135 (Jan. 2021), p. 110206. ISSN: 1364-0321. DOI: 10.1016/j.rser.2020.110206.

[7] Wu M. et al. *An integrated energy system optimization strategy based on particle swarm optimization algorithm*. In: "Energy Reports" 8 (Nov. 2022), pp. 679–691. DOI: 10.1016/j.egyr.2022.10.034.

[8] Kotzur L. et al. *A modeler's guide to handle complexity in energy systems optimization*. In: "Advances in Applied Energy" 4 (Nov. 2021), p. 100063. DOI: 10.1016/j.adapen.2021.100063.

[9] Fazlollahi S. et al. *Methods for multi-objective investment and operating optimization of complex energy systems*. In: "Energy" 45.1 (Sept. 2012), pp. 12–22. DOI: 10.1016/j.energy.2012.02.046.

[10] Salpakari J., Mikkola J., and Lund P. D. *Improved flexibility with large-scale variable renewable power in cities through optimal demand side management and power-to-heat conversion*. In: "Energy Conversion and Management" 126 (Oct. 2016), pp. 649–661. DOI: 10.1016/j.enconman.2016.08.041.

[11] Milan C. et al. *Modeling of non-linear CHP efficiency curves in distributed energy systems*. In: "Applied Energy" 148 (June 2015), pp. 334–347. DOI: 10.1016/j.apenergy.2015.03.053.

[12] Yousefi H., Ghodusinejad M. H., and Noorollahi Y. *GA/AHP-based optimal design of a hybrid CCHP system considering economy, energy and emission*. In: "Energy and Buildings" 138 (Mar. 2017), pp. 309–317. DOI: 10.1016/j.enbuild.2016.12.048.

[13] D'Ambrosio C., Lodi A., and Martello S. *Piecewise linear approximation of functions of two variables in MILP models*. In: "Operations Research Letters" 38.1 (Jan. 2010), pp. 39–46. DOI: 10.1016/j.orl.2009.09.005.

[14] Conforti M., Cornuéjols G., and Zambelli G. *Integer Programming*. Springer International Publishing, 2014. DOI: 10.1007/978-3-319-11008-0.

[15] Haimes Y. Y., Lasdon L. S., and Wismer D. A. *On a Bicriterion Formulation of the Problems of Integrated System Identification and System Optimization*. In: "IEEE Transactions on Systems, Man, and Cybernetics" SMC-1.3 (July 1971), pp. 296–297. DOI: 10.1109/tsmc.1971.4308298.

[16] Lin S. *Heuristic Programming as an Aid to Network Design*. In: "Networks" 5.1 (Jan. 1975), pp. 33–43. DOI: 10.1002/net.1975.5.1.33.

https://doi.org/10.52202/069564-0130